Investigation on exchange and correlation holes in a strongly confined electron gas

2004 J. Phys.: Condens. Matter 16 4833

(http://iopscience.iop.org/0953-8984/16/28/006)

INSTITUTE OF PHYSICS PUBLISHING JOURNAL OF PHYSICS: CONDENSED MATTER

J. Phys.: Condens. Matter **16** (2004) 4833–4844 PII: S0953-8984(04)77715-2

Investigation on exchange and correlation holes in a strongly confined electron gas

Stewart J Clark and Philip P Rushton

Department of Physics, University of Durham, Science Laboratories, South Road, Durham DH1 3LE, UK

Received 11 March 2004
Published 2 July 2004
Online at stacks.iop.org/JPhysCM/16/4833
doi:10.1088/0953-8984/16/28/006

Abstract

The nonlocal weighted density approximation (WDA) is compared with the local density approximation (LDA) and generalized gradient approximation (GGA) for a broad range of inhomogeneous electron gas densities that are confined in three dimensions (uniform confinement) and along just one dimension (non-uniform confinement), using a model external potential. All three functionals display similar properties in the uniformly confined case; however LDA and GGA energies diverge with respect to the WDA in the non-uniform strongly confined case. This is caused by the strong anisotropy in the XC hole, demonstrated by the WDA.

1. Introduction

Developing improved exchange–correlation (XC) approximations in Kohn–Sham density functional theory (KS-DFT) [1, 2] is an important area of research in quantum chemistry and condensed matter physics. One method that has received significant interest in recent years is the generalized gradient approximation (GGA) [3, 4], which builds upon the local density approximation (LDA) by including semilocal information, namely the reduced density gradient $s = |\nabla n(\mathbf{r})|/[2k_{\mathrm{F}}n(\mathbf{r})]$. Since the GGA is not a unique functional, much effort has been invested in developing optimal forms [5]. These range from first-principles derivations [6, 7]—obtained by enforcing exact conditions on the XC hole—to semi-empirical forms that are fitted to atomic and molecular data [8, 9]. As a result of this development GGAs now improve upon the LDA in several respects, and have largely become the standard XC approximation in KS-DFT calculations.

There also exist fully nonlocal approximations such as the weighted density approximation (WDA) [10, 11] and the average density approximation (ADA) [12] in which the XC energy is written as a double integral involving the density. Unfortunately these functionals have received less attention because they incur greater computational expense than the GGA. Consequently,

promising forms such as the WDA are relatively underdeveloped despite the fact that they possess several important features [13].

Whereas self-consistent properties of solid systems have been reported previously for the WDA [14], such calculations alone provide little insight at present due to the inconsistent treatment of exchange and correlation for the core electrons. It is known that using a different XC scheme for the core electrons can mask the true performance of the XC functional being tested [15]. The aim of this work is therefore to improve the understanding of the WDA by making direct comparisons with the LDA and the GGA for the inhomogeneous electron gas—a system that makes no reference to ionic cores or pseudopotentials. We investigate a wide range of density environments that vary from the weakly perturbed through to the strongly anisotropic, which are generated using a model potential that we used in a previous study [16]. In this way, the degree of anisotropy can be easily controlled. Total XC energies, E_{XC}, energy densities, e_{XC}, potentials, v_{XC}, and hole densities, $n_{\mathrm{XC}}(\mathbf{r}, \mathbf{r}')$, are calculated for the electron gas confined in three directions and along just one direction. We find that the three types of functional exhibit fairly similar properties in the uniformly confined 3D case, even when the density is strongly localized. However, in the 1D case, the properties of the LDA and GGA functionals significantly depart from those of the WDA. The XC energies from the (semi)local functionals diverge relative to the WDA, confirming previous work by Kim *et al* [17] which examined the ADA in model quasi-2D systems. The WDA XC potentials are also shallower and decay substantially more slowly than in the LDA and GGA. We show that these divergences are caused by the highly anisotropic nature of the XC hole which cannot be modelled with a (semi)local functional. This conclusion was drawn by Kim *et al* although it was not demonstrated.

In section 2 we give a brief description of the density functionals and their properties. The model potential used to obtain the densities is given in section 3. Results and conclusions are given in sections 4 and 5 respectively.

2. Details of the exchange–correlation functionals

The total spin-unpolarized XC energy E_{XC} in KS-DFT can be written generally as

$$E_{\mathrm{XC}}[n(\mathbf{r})] = \int e_{\mathrm{XC}}[n(\mathbf{r})]\,\mathrm{d}\mathbf{r}, \tag{1}$$

where we define e_{XC} as the XC energy density. The exact expression for e_{XC} is given in terms of the XC hole density $n_{\mathrm{XC}}(\mathbf{r}, \mathbf{r}')$, that is the depletion of density surrounding every electron an interacting system:

$$e_{\mathrm{XC}}[n(\mathbf{r})] = \frac{1}{2} n(\mathbf{r}) \int \frac{n_{\mathrm{XC}}(\mathbf{r}, \mathbf{r}')}{|\mathbf{r} - \mathbf{r}'|}\,\mathrm{d}\mathbf{r}'. \tag{2}$$

For an electron situated at the point $\mathbf{r}$, the XC hole density at all other points $\mathbf{r}'$ in the system is given by

$$n_{\mathrm{XC}}(\mathbf{r}, \mathbf{r}') = n(\mathbf{r}')[g_{\mathrm{XC}}(\mathbf{r}, \mathbf{r}') - 1] \tag{3}$$

where $g_{\mathrm{XC}}(\mathbf{r}, \mathbf{r}')$ is the coupling constant integral over the pair correlation function, $g^{\lambda}(\mathbf{r}, \mathbf{r}')$, with the overall density kept constant, that is

$$g_{\mathrm{XC}}(\mathbf{r}, \mathbf{r}') = \int_0^1 [g^{\lambda}(\mathbf{r}, \mathbf{r}') - 1]\,\mathrm{d}\lambda. \tag{4}$$

The XC hole obeys a normalization condition known as the XC sum rule, which preserves the charge neutrality of the electron–hole system:

$$\int n_{\mathrm{XC}}(\mathbf{r}, \mathbf{r}')\,\mathrm{d}\mathbf{r}' = -1. \tag{5}$$

The XC functionals used here are essentially direct approximations for the exact XC hole, which is unknown for inhomogeneous systems. The LDA makes two assumptions—(i) that the XC hole depends on the density at the site of the electron $n(\mathbf{r})$, not $n(\mathbf{r}')$ as in (3); (ii) that the pair correlation function is modelled by the known homogeneous electron gas function $g_{\mathrm{XC}}^{\mathrm{hom}}$. So, in the LDA the exact XC hole is approximated by

$$n_{\mathrm{XC}}(\mathbf{r}, \mathbf{r}') \approx n(\mathbf{r})(g_{\mathrm{XC}}^{\mathrm{hom}}[|\mathbf{r} - \mathbf{r}'|; n(\mathbf{r})] - 1). \tag{6}$$

Perdew and Wang [18] have devised an analytic representation of $g_{\mathrm{XC}}^{\mathrm{hom}}$ which we use in this work to generate the LDA XC holes. Since the LDA depends on the local density, relation (2) can be written simply as

$$e_{\mathrm{XC}}^{\mathrm{LDA}}[n(\mathbf{r})] = n(\mathbf{r})\epsilon_{\mathrm{XC}}^{\mathrm{hom}}[n(\mathbf{r})] \tag{7}$$

where $\epsilon_{\mathrm{XC}}^{\mathrm{hom}}[n(\mathbf{r})]$ can be decomposed into an exchange term $\epsilon_{\mathrm{X}}^{\mathrm{hom}}[n(\mathbf{r})] = -3[3\pi^2 n(\mathbf{r})]^{1/3}/(4\pi)$, and a correlation term $\epsilon_{\mathrm{C}}^{\mathrm{hom}}[n(\mathbf{r})]$ which has been determined by fitting analytic parametrizations [19] to accurate data from quantum Monte Carlo simulations of the homogeneous electron gas [20]. The LDA XC potential is obtained in the usual manner by functional differentiation of the total energy expression:

$$v_{\mathrm{XC}}^{\mathrm{LDA}}(\mathbf{r}) = \frac{\partial e_{\mathrm{XC}}^{\mathrm{LDA}}(\mathbf{r})}{\partial n(\mathbf{r})}. \tag{8}$$

A natural way to extend beyond the simple LDA is to include density gradient information. The first step along this path was made by Hohenberg, Kohn and Sham [1, 2] who proposed the generalized expansion approximation (GEA). The GEA is a second-order gradient expansion of the XC energy in which the LDA is the first-order term, and the second-order quantity involves contributions from $|\nabla n(\mathbf{r})|^2$. However, the GEA leads to very unphysical results that have been attributed to the violation of the XC sum rule (5) and the negativity constraint on the exchange hole:

$$n_{\mathrm{X}}(\mathbf{r}, \mathbf{r}') \leqslant 0 \tag{9}$$

which is another important exact condition. The GGA was constructed in order to rectify these problems by sharply terminating the GEA XC hole in real space [21, 22], so as to satisfy relations (5) and (9). The GGA XC energy can be written as a modification of the LDA with an enhancement factor $F_{\mathrm{XC}}^{\mathrm{GGA}}[r_{\mathrm{s}}, s]$ that contains the gradient information:

$$e_{\mathrm{XC}}^{\mathrm{GGA}}[n(\mathbf{r})] = e_{\mathrm{XC}}^{\mathrm{LDA}}[n(\mathbf{r})]F_{\mathrm{XC}}^{\mathrm{GGA}}[r_{\mathrm{s}}, s] \tag{10}$$

where $r_{\mathrm{s}} = [4/3\pi n(\mathbf{r})]^{1/3}$ is the Wigner–Seitz radius. The GGA XC potential can be evaluated using the expression

$$v_{\mathrm{XC}}^{\mathrm{GGA}}(\mathbf{r}) = \frac{\partial e_{\mathrm{XC}}^{\mathrm{GGA}}(\mathbf{r})}{\partial n(\mathbf{r})} - \nabla \cdot \frac{\partial e_{\mathrm{XC}}^{\mathrm{GGA}}(\mathbf{r})}{\partial \nabla n(\mathbf{r})}. \tag{11}$$

Unfortunately an explicit local XC hole like that for the LDA in relation (6) cannot be obtained within the GGA. System and spherical averaged XC holes can be obtained in the GGA [23]; however, this procedure effectively smooths out the nonlocalities in the true XC hole, which become a dominant factor in strongly inhomogeneous systems, like the ones studied here. There is no definition of a local hole in the GGA and so it is not possible to compare GGA energy densities, as it is possible to add a quantity to (10) that modifies $e_{\mathrm{XC}}^{\mathrm{GGA}}$ locally but leaves $E_{\mathrm{XC}}^{\mathrm{GGA}}$ unchanged. Such a quantity could take the form of the divergence of a vector field that integrates to zero. Consequently we will calculate total XC energies and potentials using a popular non-empirical GGA known as PBE [7].

Whereas the GGA is based upon the LDA, the WDA derives from the exact e_{XC} by making the analytic approximation [24] $[g(\mathbf{r},\mathbf{r}')-1] \approx G_{\mathrm{XC}}^{\mathrm{WDA}}[|\mathbf{r}-\mathbf{r}'|;\tilde{n}(\mathbf{r})]$, so that equation (2) becomes

$$e_{\mathrm{XC}}^{\mathrm{WDA}}[n(\mathbf{r})] = \frac{1}{2}n(\mathbf{r})\int n(\mathbf{r}')\frac{G_{\mathrm{XC}}^{\mathrm{WDA}}[|\mathbf{r}-\mathbf{r}'|;\tilde{n}(\mathbf{r})]}{|\mathbf{r}-\mathbf{r}'|}\,\mathrm{d}\mathbf{r}', \tag{12}$$

where the weighted density parameter, $\tilde{n}(\mathbf{r})$, is a nonlocal quantity fixed at every point in space by the XC sum rule (5). We examined a range of functions for $G_{\mathrm{XC}}^{\mathrm{WDA}}[|\mathbf{r}-\mathbf{r}'|;\tilde{n}(\mathbf{r})]$ in a previous study [13] and found that a particularly effective form is that of a simple Gaussian:

$$G_{\mathrm{XC}}^{\mathrm{WDA}}[|\mathbf{r}-\mathbf{r}'|;\tilde{n}(\mathbf{r})] = \alpha[\tilde{n}(\mathbf{r})]\mathrm{e}^{-\beta(\tilde{n})|\mathbf{r}-\mathbf{r}'|^2}. \tag{13}$$

Consequently we will adopt this function here. The parameters $\alpha(\tilde{n})$ and $\beta(\tilde{n})$ are obtained by fulfilling equations (2) and (5) for a homogeneous electron gas of density $n = n(\mathbf{r})$. The WDA XC energy density $e_{\mathrm{XC}}^{\mathrm{WDA}}$ and XC hole density, $n_{\mathrm{XC}}^{\mathrm{WDA}}(\mathbf{r},\mathbf{r}') = n(\mathbf{r}')G_{\mathrm{XC}}^{\mathrm{WDA}}$, are uniquely defined and will be compared with those of the LDA.

Although we do not generate self-consistent densities with the WDA, we will compare the XC potentials for all three functionals evaluated using LDA densities. The WDA XC potential is given by

$$\begin{aligned} v_{\mathrm{XC}}^{\mathrm{WDA}}(\mathbf{r}) = \epsilon_{\mathrm{XC}}(\mathbf{r}) &+ \frac{1}{2}\int n(\mathbf{r}')\frac{G_{\mathrm{XC}}^{\mathrm{WDA}}[|\mathbf{r}-\mathbf{r}'|;\tilde{n}(\mathbf{r}')]}{|\mathbf{r}-\mathbf{r}'|}\,\mathrm{d}\mathbf{r}' \\ &+ \frac{1}{2}\int \mathrm{d}\mathbf{r}''\int \frac{n(\mathbf{r}')n(\mathbf{r}'')}{|\mathbf{r}'-\mathbf{r}''|}\frac{\delta G_{\mathrm{XC}}^{\mathrm{WDA}}[|\mathbf{r}'-\mathbf{r}''|;\tilde{n}(\mathbf{r}')\,]}{\delta n(\mathbf{r})}\,\mathrm{d}\mathbf{r}'. \end{aligned} \tag{14}$$

It is again clear that the WDA is very different from its (semi)local counterparts for the XC potential. A notable feature of this XC potential is that it decays as $-1/(2r)$ at large distance from an isolated density distribution, compared with the exact $-1/r$ result. However, an exception to this is for atomic hydrogen and helium whereby the WDA spin-dependent potential decays in the same way as the exact potential.

We have implemented the WDA within a periodic code [25] since the real-space integral equations can be most effectively computed in reciprocal space (by exploiting the convolution theorem) and efficiently transformed using fast Fourier transform algorithms. The details of the implementation are described in [13].

3. The model system

The electron gas densities are generated self-consistently using KS-DFT with the single-particle Hamiltonian

$$H = -\tfrac{1}{2}\nabla^2 + v_{\mathrm{ext}}(\mathbf{r}) + v_{\mathrm{H}}(\mathbf{r}) + v_{\mathrm{XC}}^{\mathrm{LDA}}(\mathbf{r}), \tag{15}$$

where the first term is the kinetic energy and $v_{\mathrm{H}}(\mathbf{r})$ and $v_{\mathrm{XC}}(\mathbf{r})$ are the Hartree and LDA exchange–correlation potentials respectively. The external potential $v_{\mathrm{ext}}(\mathbf{r})$ is modelled by

$$v_{\mathrm{ext}}(\mathbf{r}) = v_0\cos\left[\frac{2\pi}{a_0}(q_x x)\right]\cos\left[\frac{2\pi}{a_0}(q_y y)\right]\cos\left[\frac{2\pi}{a_0}(q_z z)\right], \tag{16}$$

where a_0 is the unit cell parameter. This allows a simple way of controlling the density inhomogeneity through the choice of wavevector components $q_{x,y,z}$ and amplitude v_0. In this study, we analyse the effect of applying one period of the cosine potential in three dimensions, where $q_{x,y,z} = (1,1,1)$, and in just one dimension, where $q_{x,y,z} = (1,0,0)$. This yields densities with a single maximum along the length of a unit cell in either one or three directions, which we refer to as non-uniform and uniform confinement respectively.

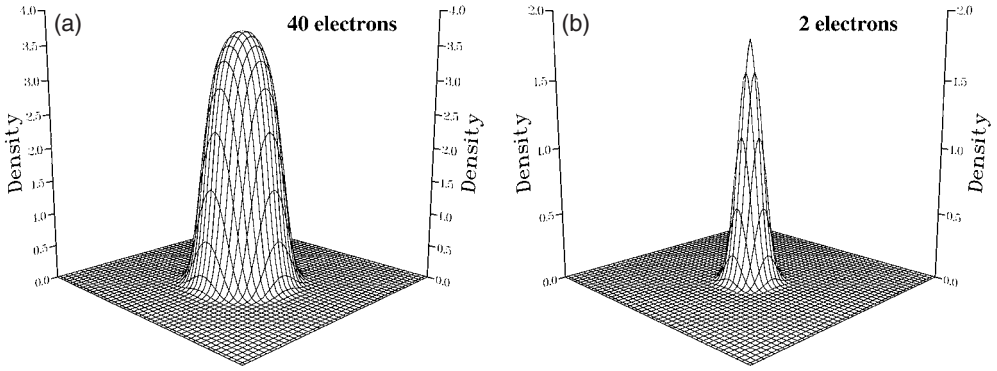

Figure 1. Uniformly confined densities shown in a plane taken through the centre of the confining potential with $v_0 = v_0^{\max}$, for (a) the $r_s = 1.51a_0$ and (b) $r_s = 4.31a_0$ systems.

Table 1. The total exchange–correlation energy E_{XC}^{WDA}/N, and the difference relative to the LDA and the GGA for the uniformly confined system with $r_s = 1.51a_0$.

v_q/ϵ_F^0	E_{XC}^{WDA}/N	$\Delta E_{XC}^{LDA}/N$	$\Delta E_{XC}^{GGA}/N$
1.4	−0.3660	−0.0032 (−0.8%)	−0.0034 (−0.9%)
2.7	−0.4209	−0.0005 (−0.1%)	−0.0024 (−0.6%)
13	−0.6898	+0.0053 (+0.8%)	−0.0063 (−0.7%)
41	−0.9425	+0.0071 (+0.8%)	−0.0061 (−0.7%)
274	−1.0362	+0.0099 (+0.9%)	−0.0056 (−0.5%)

The inhomogeneity in the system (which we characterize by the full width at half-maximum (FWHM)) is therefore determined by the amplitude v_0. A large value of v_0 on the scale of the Fermi energy $\epsilon_0 = (k_F^0)^2/2$, where $k_F^0 = (3/4\pi r_s^3)$ is the Fermi wavevector, gives rise to a narrow density profile and therefore a small FWHM. In each case we consider v_0 increased up to some maximum value $v_0^{\max}$ (corresponding to the most strongly inhomogeneous regime) such that any further increases in v_0 yield negligible changes in the self-consistent density.

The 1D version of this potential was employed in a previous study by Nekovee *et al* [26] using the variational Monte Carlo (VMC) method. Interestingly, they found that differences between the LDA and the VMC XC energy densities closely followed the Laplacian of the corresponding density $\nabla^2 n(\mathbf{r})$, in magnitude, shape and sign. In subsequent work [16] we performed similar calculations with the WDA and found that XC energy differences with the LDA exhibited the same link with $\nabla^2 n(\mathbf{r})$, in good agreement with the VMC findings. We will investigate this property for a broader range of density inhomogeneity.

4. Results

4.1. Uniform confinement

For the case of uniform confinement, we consider systems with high ($r_s = 1.52a_0$) and low average density ($r_s = 4.31a_0$), containing $N = 40$ and 2 electrons in the unit cell respectively. The most strongly confined densities are obtained with $v_0^{\max} = 274\epsilon_F^0$ and $2016\epsilon_F^0$ for the high and low density systems respectively. Shown in figure 1 are the densities obtained when $v_0 = v_0^{\max}$.

XC energy differences for the LDA and GGA relative to the WDA, $\Delta E_{XC}^{LDA,GGA}/N = (E_{XC}^{LDA,GGA} - E_{XC}^{WDA})/N$, are given in table 1, for the high density case, and table 2, for the

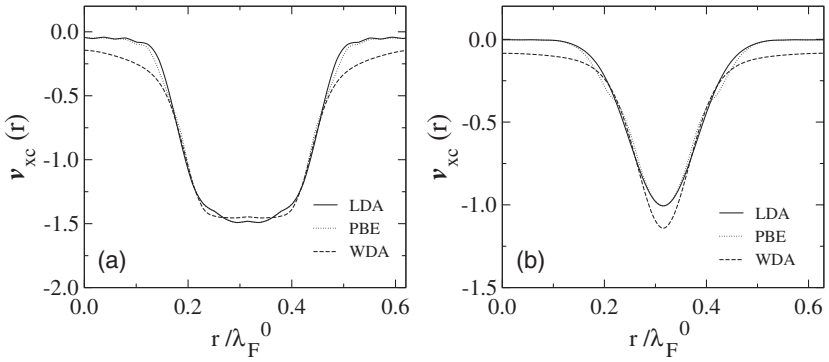

Figure 2. Exchange–correlation potentials $v_{\mathrm{XC}}(\mathbf{r})$ taken through the centre of uniformly confined densities, with (a) $v_{\mathrm{q}} = 41\epsilon_{\mathrm{F}}^0$ and (b) $v_{\mathrm{q}} = 303\epsilon_{\mathrm{F}}^0$.

Table 2. The total exchange–correlation energy $E_{\mathrm{XC}}^{\mathrm{WDA}}/N$, and the difference relative to the LDA and the GGA for the uniformly confined system with $r_{\mathrm{s}} = 4.31a_0$.

$v_{\mathrm{q}}/\epsilon_{\mathrm{F}}^0$	$E_{\mathrm{XC}}^{\mathrm{WDA}}/N$	$\Delta E_{\mathrm{XC}}^{\mathrm{LDA}}/N$	$\Delta E_{\mathrm{XC}}^{\mathrm{GGA}}/N$
2.0	−0.3321	+0.0336 (+10%)	+0.0230 (+7%)
20	−0.4042	+0.0452 (+11%)	+0.0305 (+8%)
101	−0.6155	+0.0740 (+11%)	+0.0455 (+7%)
303	−0.7789	+0.0935 (+12%)	+0.0534 (+7%)
2016	−0.8831	+0.1053 (+12%)	+0.0581 (+7%)

low density system, for a range of v_0. In the high density case, $\Delta E_{\mathrm{XC}}^{\mathrm{LDA}}/N$ changes sign from negative to positive on going to the more strongly confined densities, and vanishes near the middle of the density range. In contrast, the GGA differences are all negative, and actually become smaller as v_0 increases. So for moderate to high values of v_0, the WDA lies between the LDA and the GGA energies. At low density, although the energy differences are significantly greater than in the high density case, they do not appear to be affected by the change in inhomogeneity, since the deviations are remarkably constant for both functionals. Although they may be purely coincidental, the differences may be a result of self-interaction errors within the LDA and GGA which become more predominant in low density systems. XC energy density differences between the LDA and the WDA do not bear any resemblance to the Laplacian of the density in the uniformly confined densities studied here.

Examples of the XC potential for each functional are given in figure 2 in the high and low density systems. The LDA and GGA potentials are largely indistinguishable for both cases. At high density, the WDA potential is similar to the (semi)local functionals when the density is large; however, there is a substantial difference in the tail regions of the density, where the WDA decays substantially more slowly due to its $-1/(2r)$ behaviour, compared with the faster exponential decay of the LDA and GGA potentials. In the low density case, the WDA potential is also deeper around the density maximum.

4.2. Non-uniform confinement

Now we consider the effect of non-uniform confinement on systems with average density $r_{\mathrm{s}} = 2a_0$ and $4.3a_0$ containing $N = 20$ and 2 electrons respectively; examples of the full range of density distributions are shown in figure 3. In figure 4 we present differences in the total XC

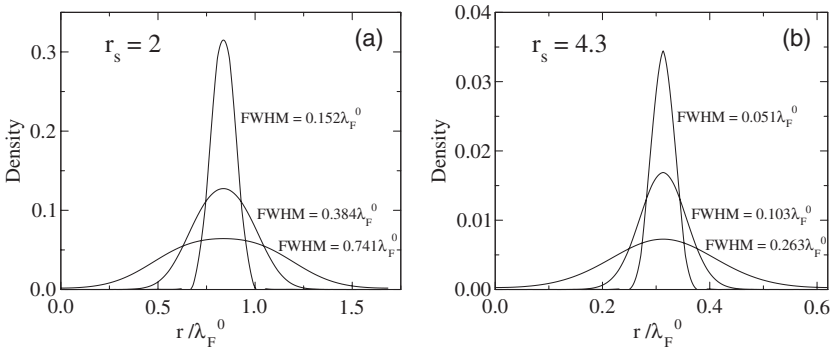

Figure 3. Examples of the non-uniform densities obtained for (a) the $r_s = 2a_0$ system, ranging from the most weakly confined (FWHM $= 0.741\lambda_F^0$) to the most strongly confined (FWHM $= 0.152\lambda_F^0$), and similarly for (b) the $r_s = 4.3a_0$ system. The distance along the direction of inhomogeneity r is given in terms of the Fermi wavelength $\lambda_F^0 = 2\pi/k_F^0$.

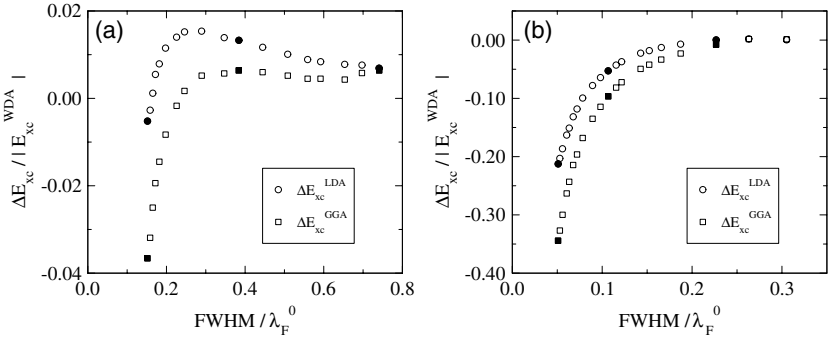

Figure 4. Total XC energy differences per electron $\Delta E_{\rm XC}/N$ relative to the WDA for the LDA (circles) and GGA (boxes) at (a) $r_s = 2a_0$ and (b) $r_s = 4.3a_0$, as a function of the FWHM of the non-uniform density profiles. The shaded data points correspond to the densities shown in figure 2.

energy per electron relative to the WDA for the LDA ($\Delta E_{\rm XC}^{\rm LDA}/N$) and the GGA ($\Delta E_{\rm XC}^{\rm GGA}/N$) for a range of density profiles. In the $r_s = 2a_0$ system, shown in figure 4(a), the LDA and GGA deviations are positive for small and intermediate confinements, with the GGA in closer agreement with the WDA. As the confinement gets stronger, the GGA differences are almost constant whereas for the LDA they steadily increase, reaching a maximum when the FWHM is $\sim 0.25\lambda_F^0$. For stronger confinement, the differences become negative and start to diverge for both functionals; however, the GGA diverges faster than the LDA. The same divergent behaviour is observed in the low density case given in figure 4(b), except that the densities are more strongly confined on the scale of λ_F^0, so the energy differences are much greater than in the high density case. Self-interaction errors will also contribute to the differences. These results are consistent with the findings of Kim *et al* [17] who found that the nonlocal ADA gives very accurate energies in the strong 2D limit, whereas (semi)local functionals diverge to minus infinity.

Analysing the XC energy density locally we find that the energy difference $\Delta e_{\rm XC} = e_{\rm XC}^{\rm LDA} - e_{\rm XC}^{\rm WDA}$, plotted along the line of inhomogeneity, bears little resemblance to the Laplacian of the density $\nabla^2 n(r)$ for weak confinement (figure 5). However, for intermediately confined

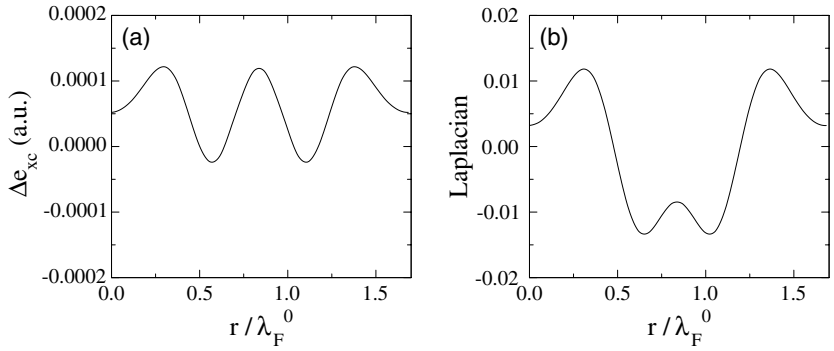

Figure 5. The XC energy density difference Δe_{XC} between the LDA and the WDA (a), and the Laplacian of the density $\nabla^2 n(r)$ (b), along the direction of inhomogeneity for a non-uniformly confined density with FWHM $= 0.741\lambda_{\mathrm{F}}^0$.

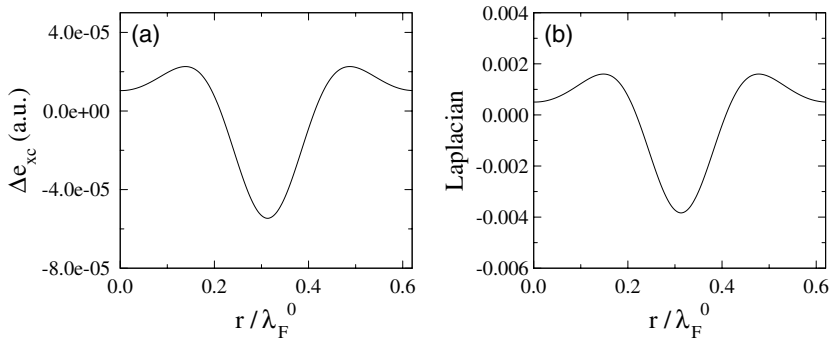

Figure 6. The same as in figure 5, but with FWHM $= 0.227\lambda_{\mathrm{F}}^0$.

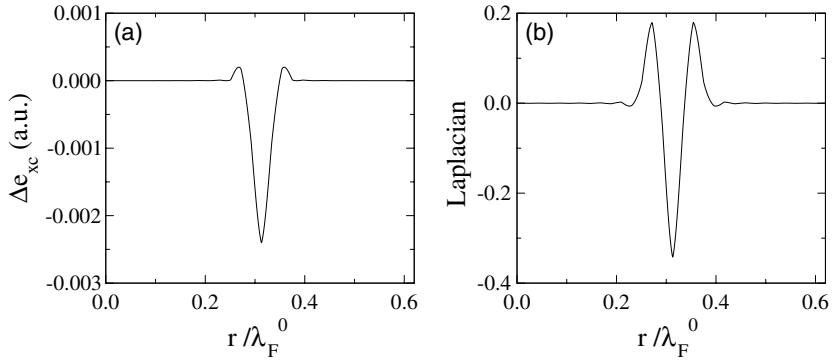

Figure 7. The same as in figure 5, but with FWHM $= 0.053\lambda_{\mathrm{F}}^0$.

densities, Δe_{XC} and $\nabla^2 n(r)$ are strikingly similar, as shown in figure 6. When the density is strongly confined, Δe_{XC} becomes large and negative near the density maximum in comparison to $\nabla^2 n(r)$ (see figure 7). This last result is in accordance with the work of Garcia-Gonzalez [27] who showed that $e_{\mathrm{XC}}^{\mathrm{LDA}} \to -\infty$ when the dimensionality of an electron gas changes from 3D to 2D.

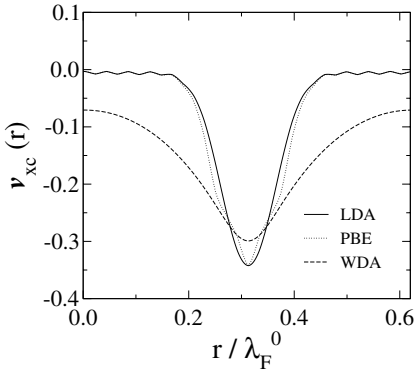

Figure 8. Exchange–correlation potentials $v_{\mathrm{XC}}(r)$ along the direction of inhomogeneity for a density with FWHM $= 0.068\lambda_{\mathrm{F}}^{0}$.

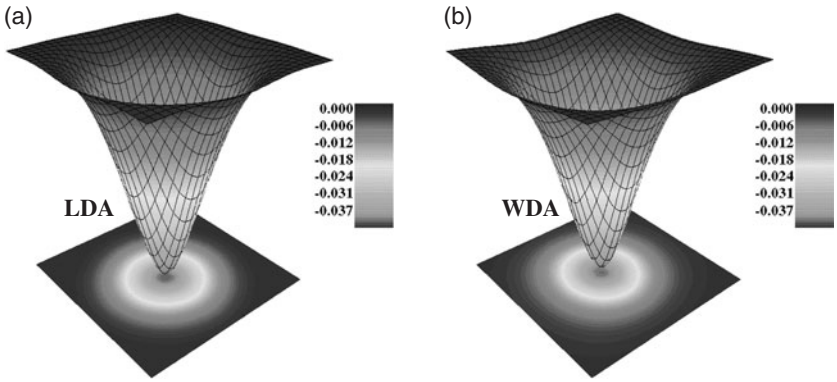

Figure 9. Exchange–correlation holes $n_{\mathrm{XC}}(\mathbf{r}, \mathbf{r}')$ surrounding an electron at the density maximum for the non-uniformly confined density with FWHM $= 0.741\lambda_{\mathrm{F}}^{0}$, obtained using (a) the LDA and (b) the WDA.

The WDA XC potential in the non-uniform case is vastly different from the LDA and GGA XC potentials in the strongly confined regime, which again only exhibit small differences from each other. This is clearly shown in figure 8 for a density with FWHM $= 0.068\lambda_{\mathrm{F}}$. It should be noted that the wiggles in the GGA potential at positions of low density are a consequence of the parametrization used to construct $F_{\mathrm{XC}}^{\mathrm{GGA}}$ [28], although the LDA exhibits the same spurious behaviour. The much shallower and more slowly decaying potential exhibited by the WDA may have important implications for the description of subband energy levels in real quasi-2D systems such as inversion and accumulation layers in metal–oxide–semiconductor systems, which from a modelling viewpoint are similar to the strongly confined densities examined here. The LDA is known to overestimate these levels in comparison to experiment [29, 30], and a shallower potential like that obtained with the WDA is likely to provide an improvement.

Finally, we compare XC holes $n_{\mathrm{XC}}(\mathbf{r}, \mathbf{r}')$ using the LDA and the WDA, when an electron is located at the density maximum. When the density is sufficiently slowly varying, the WDA hole is almost exactly spherical; consequently the LDA is in very good agreement as shown in figure 9. However, as the confinement gets stronger, the WDA hole becomes increasingly anisotropic as it contracts in the direction of density inhomogeneity. Since the

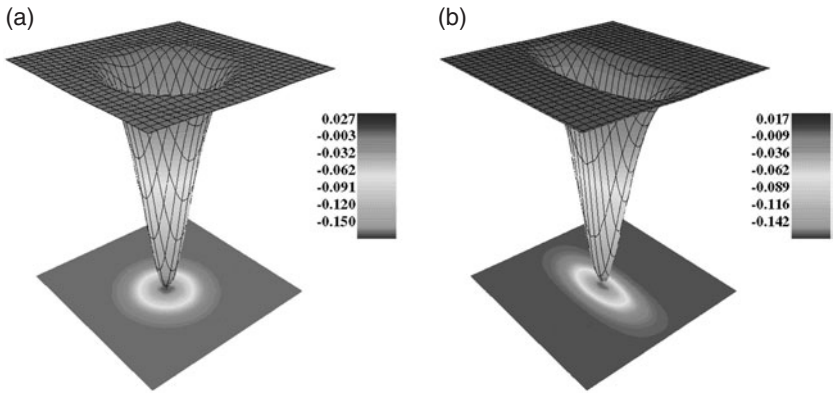

Figure 10. The same as in figure 9, but for a density with FWHM $= 0.152\lambda_F^0$.

LDA hole depends on the local density, which in this case is the value at the peak in the density profile, the LDA hole remains spherical and continues to get deeper relative to the WDA as the confinement, and hence the local density at the maximum, increases (shown in figure 10). This accounts for the divergent nature of the LDA energy densities, since ϵ_{XC} is directly related to the on-top hole density $n_{XC}(r, r)$ through relation (2). Although GGA holes cannot be calculated, a similar explanation for the divergence of the GGA energies can be given as follows: the major contribution to the XC energy in the strongly confined regime is from exchange; this is reflected by the correlation enhancement factor F_C^{GGA} which turns off for values of $s \sim> 4$. So we need only consider the form of F_X^{GGA}. Now, the cut-off radius in real space for the numerical GGA exchange hole reduces as $s \to \infty$ (see figure 2 of [23]); consequently the hole becomes highly localized around the electron, and the on-top value gets deeper (more negative) because of the XC sum rule. As a result, $F_X^{GGA} \geqslant 1$ for all s[Note 1] which causes the GGA energies to be lower than in the LDA. This adds to the LDA divergence and accounts for why the GGA is worse than the LDA for strong confinement. In contrast, the nonlocal dependence on the density in the WDA allows its XC hole to distort and spread along the ridge of the density profile, resulting in shallower holes and XC energy densities that tend to finite values in the strongly confined limit. A striking example of this anisotropy is illustrated in figure 11 for the most strongly confined density (on the scale of λ_F^0) in this study. It is clear that the WDA hole correctly takes on the same quasi-2D character as the density profile shown in figure 2(b). The WDA hole can also be highly nonlocal in this system. When the electron moves parallel to the direction of inhomogeneity, into the low density region midway between density peaks, the hole stays located at the density maximum completely delocalized from the electron.

We have made attempts to counteract the GGA divergence, whilst maintaining its properties for conventional systems, by modifying F_X^{GGA} such that it becomes increasingly negative for $s \geqslant 4$. We find that it is impossible to collectively improve total XC energies relative to the WDA at all confinement strengths shown in figure 4(b). Present meta-GGA functionals [31] which include additional semilocal information beyond the GGA level are also unable to rectify the divergence [32]. In fact Kim *et al* found that they worsen the performance of the GGA.

[1] The exchange enhancement factor for the PW91 GGA becomes less than 0 for s greater than ∼8. Consequently PW91 is a slight improvement on the PBE-GGA in strong confinement.

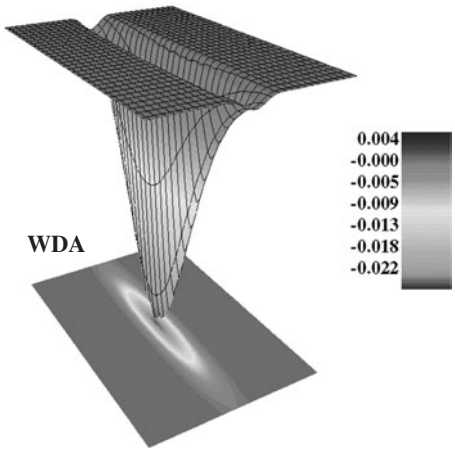

Figure 11. The exchange–correlation hole obtained using the WDA for the most strongly confined density with FWHM $= 0.051\lambda_{\mathrm{F}}^{0}$.

5. Conclusions

We have analysed the performance of the nonlocal WDA for a range of density inhomogeneities in the electron gas, that vary from weak to strong anisotropy, with different dimensional characters. Total XC energies are very close to those of the (semi)local functionals, especially in the high density, uniformly confined regime. This is encouraging for the WDA since this is an environment that is known to be successfully described by (semi)local functionals, even when the density is significantly localized. Substantial differences arise between the nonlocal and (semi)local XC descriptions when the density is strongly confined in one dimension. With regard to the XC potential, it is clear that the WDA description differs from the (semi)local functionals in all of the density regimes examined; again the most prominent changes occur for the non-uniform case. It is also interesting to note that the GGA only modifies the LDA potential by a small amount in all cases considered.

The successful description of key XC quantities in the range of density inhomogeneities examined here demonstrates the universal nature of the WDA. Consequently we hope that this work will encourage greater interest in the WDA, both in its development and in applications.

Acknowledgment

PPR thanks the EPSRC for financial support.

References

[1] Hohenberg P and Kohn W 1964 *Phys. Rev.* **136** B864
[2] Kohn W and Sham L J 1965 *Phys. Rev.* **140** A1133
[3] Langreth D C and Perdew J P 1980 *Phys. Rev.* B **21** 5469
[4] Langreth D C and Mehl M J 1983 *Phys. Rev.* B **28** 1809
[5] Perdew J P and Burke K 1996 *Int. J. Quantum Chem.* **57** 309
[6] Perdew P J 1991 *Electronic Structure of Solids '91* ed P Ziesche and H Eschrig (Berlin: Akademie)
Perdew J P, Chevary J A, Vosko S H, Jackson K A, Pederson M R, Singh D J and Fiolhais C 1992 *Phys. Rev.* B **46** 6671
[7] Perdew J P, Burke K and Ernzerhof M 1996 *Phys. Rev. Lett.* **77** 3865

[8] Becke A D 1988 *Phys. Rev.* A **38** 3098
[9] Hamprecht F A, Cohen A J, Tozer D J and Handy N C 1998 *J. Chem. Phys.* **109** 6264
[10] Alonso J A and Girifalco L A 1976 *Phys. Rev.* B **17** 3735
[11] Gunnarsson O, Jonson M and Lundqvist B I 1977 *Solid State Commun.* **24** 765
[12] Gunnarsson O, Jonson M and Lundqvist B I 1979 *Phys. Rev.* B **20** 3136
[13] Rushton P P, Tozer D J and Clark S J 2002 *Phys. Rev.* B **63** 235203
[14] Singh D J 1993 *Phys. Rev.* B **48** 14099
[15] Rushton P P, Clark S J and Tozer D J 2001 *Phys. Rev.* B **63** 115206
[16] Rushton P P, Tozer D J and Clark S J 2002 *Phys. Rev.* B **65** 193106
[17] Kim Y, Lee I, Nagaraja S, Leburton J P, Hood R Q and Martin R M 2000 *Phys. Rev.* B **61** 5202
[18] Perdew J P and Wang Y 1992 *Phys. Rev.* B **46** 12947
Perdew J P and Wang Y 1997 *Phys. Rev.* B **56** 7018
[19] Perdew J P and Zunger A 1981 *Phys. Rev.* B **23** 5048
[20] Ceperley D M and Alder B J 1980 *Phys. Rev. Lett.* **45** 566
[21] Perdew J P and Wang Y 1985 *Phys. Rev. Lett.* **55** 1665
Perdew J P and Wang Y 1985 *Phys. Rev. Lett.* **55** 2370 (erratum)
[22] Perdew J P and Wang Y 1986 *Phys. Rev.* B **33** 8800
Perdew J P and Wang Y 1989 *Phys. Rev.* B **40** 3399
[23] Perdew P J, Burke K and Wang Y 1996 *Phys. Rev.* B **54** 16533
[24] Gunnarsson O and Jones R O 1980 *Phys. Scr.* **21** 394
[25] The CASTEP code: Segall M D, Lindan P J D, Probert M J, Pickard C J, Hasnip P, Clark S J and Payne M C 2002 *J. Phys.: Condens. Matter* **14** 2717
[26] Nekovee M, Foulkes W M C and Needs R J 2001 *Phys. Rev. Lett.* **87** 036401
[27] Garcia-Gonzalez P 2000 *Phys. Rev.* B **62** 2321
[28] Filippi C, Umrigar C J and Taut M 1994 *J. Chem. Phys.* **100** 1290
[29] Vinter B 1979 *Phys. Rev.* B **20** 2395
[30] Ando T, Fowler A B and Stern F 1982 *Rev. Mod. Phys.* **54** 437
[31] Perdew J P, Kurth S, Zupan A and Blaha P 1999 *Phys. Rev. Lett.* **82** 2544
Perdew J P, Kurth S, Zupan A and Blaha P 1999 *Phys. Rev. Lett.* **82** 5179
[32] Pollack L and Perdew J P 2000 *J. Phys.: Condens. Matter* **12** 1239